THE JOURNAL OF PHYSICAL CHEMISTRY B

Article

pubs.acs.org/JPCB

Interplay Between π-Stacking and Hydrogen Bonding in the Self-Association of Different Isomers of Naphthalenedicarboxylic Acid

Paul D. Greenstein[†,‡] and Leah B. Casabianca*[,†]

[†]Department of Chemistry, Clemson University, Clemson, South Carolina 29634, United States

Supporting Information

ABSTRACT: Using proton and carbon chemical shifts, we investigated the self-association of three isomers of naphthalenedicarboxylic acid, a model for the aggregation of asphaltenes. Experimental proton chemical shifts of each isomer were measured as a function of concentration in an aprotic solvent. Several potential structures of the monomer and dimer of each naphthalenedicarboxylic acid were considered, and calculated proton chemical shifts for the potential monomer and dimer structures were compared to the experimental chemical shifts to find the weighted average structure that best fit the experimental shifts. Calculated carbon chemical shifts were also compared to experimental values. The chemical shift comparison and calculated energies indicate that π-stacked dimers are not likely to contribute significantly to the dimer structure of any of the three naphthalenedicarboxylic acid isomers studied.

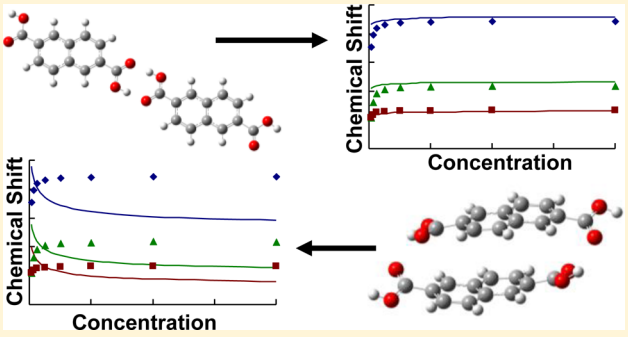

INTRODUCTION

Aromatic carboxylic acids are important starting materials for the synthesis of metal−organic frameworks (MOFs)[1−7] and metal−organic coordination complexes[8−13] and for use in crystal engineering.[14,15] The variety of positions of the dicarboxylic acids that are available, often commercially, makes this kind of molecule an ideal synthetic building block. Substituted naphthalenes also have importance as model compounds for asphaltene, the heavy component of crude oil.[16]

The self-association of aromatic carboxylic acids is important to study. Self-association in solution can lead to aggregation, reduce bioavailability, and alter the optical properties of molecules. Self-association is also related to nucleation and crystal formation. In this work, we explore the factors behind self-association in three isomers of naphthalenedicarboxylic acid. Because the formation of carboxylic acid dimers is well-known, we expect hydrogen bonding between carboxylic acid groups to be a major factor in the self-association of these compounds. Additionally, polycyclic aromatic hydrocarbons (PAH) such as naphthalene and anthracene are also known to form π-stacked dimers. In the present work, we aim to deduce the relative importance of these two factors, hydrogen bonding and π-stacking, in naphthalenedicarboxylic acids. These results are important in understanding aggregation of asphaltenes, when using high concentrations of similar compounds for synthesis of metal−organic complexes, and in directing crystal growth of this kind of compound when used in crystal engineering.

π−π interactions are related to crystal packing, aromatic molecules interacting with carbon nanotubes and graphene,[17] intercalation of molecules between DNA bases,[18,19] and stabilization of protein structures due to π−π interactions between aromatic residues.[20] Despite the importance of π−π interactions, they are still not well understood.[21−28] One of the difficulties in studying π−π interactions by computational methods is that these interactions are dominated by dispersion interactions.[29] Dispersion interactions are not accounted for in density functional theory (DFT), a popular method due to its ability to achieve high accuracy with relatively little computational cost. Aggregation of aromatic compounds due to π-stacking has been investigated by both solution-state[30−44] and solid-state[45−54] NMR. In particular, solid-state ^{1}H NMR methods have been used to elucidate the interplay between π-stacking and hydrogen bonding contributions to the dimerization of a carboxylic acid derivative of hexabenzocoronene.[55]

In this work, we considered the self-association of three structural isomers of naphthalenedicarboxylic acid (see Figure 1) in deuterated dimethyl sulfoxide (DMSO-d_6). Self-association was clearly seen by measuring changes in proton chemical shifts as a function of naphthalenedicarboxylic acid concentration. We then calculated the chemical shifts for several monomer and dimer structures of each naphthalenedicarboxylic acid to determine which dimer structures lead to chemical shifts that best agree with experiment. Dimers that represent carboxylic acid dimer formation and dimers that incorporated both π-stacking and carboxylic acid dimer formation were considered. The degree of agreement between

Received: February 14, 2017
Revised: April 26, 2017
Published: May 10, 2017

DOI: 10.1021/acs.jpcb.7b01465
J. Phys. Chem. B 2017, 121, 5086−5093

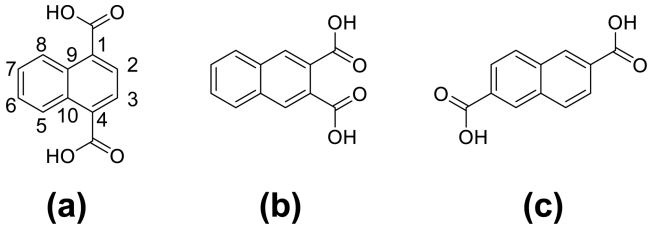

Figure 1. Chemical structures of the three isomers of naphthalenedicarboxylic acid considered in this work: (a) 1,4-naphthalenedicarboxylic acid, (b) 2,3-naphthalenedicarboxylic acid, and (c) 2,6-naphthalenedicarboxylic acid. Standard naphthalene proton/carbon numbering is shown in structure a.

chemical shifts calculated for each potential dimer structure and the experimental chemical shifts allowed us to determine the relative importance of π-stacking and carboxylic acid dimer formation in these naphthalenedicarboxylic acids.

EXPERIMENTAL METHODS

Naphthalenedicarboxylic acids were purchased from Sigma-Aldrich, Inc. (St. Louis, MO, United States). Deuterated dimethyl sulfoxide was purchased from Fisher Scientific (Hampton, NH, United States). Samples were made by weighing out the appropriate amount of each acid to make 40 mM, and subsequent samples at lower concentrations were made by serial dilution. DMSO was chosen as the solvent to avoid complications due to different protonation states of the carboxylic acid groups. A small amount of trimethylsilylpropanoic acid (TSP, Sigma-Aldrich) was added to the DMSO solution for chemical shift referencing.

^{1}H NMR spectra were collected on a JEOL Eclipse+500 MHz spectrometer operating at 500.15992 MHz. Spectra were collected with a spectral width of 7507.51 Hz and 16 384 data points and zero-filled to 65 536 points for a digital resolution of 0.11 Hz/point. All ^{1}H NMR measurements were made at room temperature in the absence of variable temperature control. ^{1}H NMR shifts were referenced to TSP at 0.000 ppm. ^{13}C NMR spectra were collected on a 600 MHz Varian/Agilent DD2 spectrometer operating at a ^{13}C frequency of 150.8185987 MHz with a 3 mm HCN coldprobe at the Complex Carbohydrate Research Center at the University of Georgia. A spectral width of 37 878.8 Hz was used, and 65 536 points were collected and zero-filled to 757 576 for a digital resolution of 0.05 Hz. ^{13}C chemical shifts were referenced to the DMSO solvent peak at 39.500 ppm. Carbon peak assignments were made by assigning the protonated carbons based on heteronuclear multiple quantum coherence (HMQC)[56] spectra. For the HMQC spectra, 64 scans with 16 dummy scans and between 78 and 256 t_1 increments were collected. Spectral widths of 15−16 ppm in the ^{1}H dimension and 150−180 ppm in the ^{13}C dimension were used. The recycle delay was 2 s. The two aromatic nonprotonated carbons were assigned based on calculated chemical shifts.

COMPUTATIONAL METHODS

All calculations were done with the Gaussian 09 program.[57] Geometry optimizations of monomer and dimer structures were done at the B3LYP/6-31G* level of theory.[58−60] Frequency calculations were then performed on the optimized structures at the same level of theory to ensure that all geometry-optimized structures were in fact local minima, as indicated by the absence of imaginary vibrational frequencies. Single-point energy calculations and chemicals shift calculations were then performed on these geometry-optimized structures using B3LYP/6-311G[58,59,61] with the gauge-including atomic orbitals (GIAO) method[62] for calculation of chemical shifts. Solvent effects were included in all calculations using the polarizable continuum model (PCM)[63−66] with dimethyl sulfoxide as the solvent.

Calculated chemical shielding values were converted to chemical shifts using the following equation:

$$\delta = \sigma_{ref} - \sigma \quad (1)$$

where δ is the chemical shift, σ is the calculated shielding, and σ_{ref} is a reference shielding, equal to the shielding of a reference compound that is taken to be 0 ppm on the experimental chemical shift scale. In this work, σ_{ref} for ^{1}H was taken to be a variable parameter in the data fitting. This was done to minimize the dependence of the results on the choice of reference, since the chemical shift difference between the monomer and dimer is always independent of the value chosen for the chemical shift reference. For the ^{13}C nucleus, a value of 183.2 ppm was used for σ_{ref}. This value corresponds to the calculated shielding of ^{13}C in TMS, using benzene as an indirect reference compound. The shielding of benzene was calculated at the same level of theory and with the same solvent model as the naphthalenedicarboxylic acid chemical shifts and was added to the experimental chemical shift of benzene as a trace impurity in DMSO, 128.3 ppm.[67] Using benzene as an indirect reference has been shown to lead to better agreement between calculated and experimental chemical shifts for aromatic carbons than calculating the shielding of TMS directly.[68,69] This was also seen to be the case in the current work. The value of 183.2 ppm for σ_{ref} that we used in the current work led to better agreement with experiment than the value for σ_{ref} that we obtained by calculating the shielding of TMS in DMSO solvent directly (190.4 ppm). Using the value for σ_{ref} that was determined using benzene as an indirect reference gives a very good agreement between experiment and calculated chemical shifts, especially for the aromatic naphthalene carbons.

Conformational Space Sampling. Conformational space was sampled by rotating about the (C“)C—C(=O) bond. Geometry optimizations were performed for monomers with starting configurations having C“C—C=O dihedral angles ranging from 0 to 360° in 10° increments. From these calculations, six local minima were found for the monomer of 1,4-naphthalenedicarboxylic acid, and three local minima each were found for the monomers of 2,3-naphthalenedicarboxylic acid and 2,6-naphthalenedicarboxylic acid. The structures of these local minima, along with the dihedral angles, are shown in Figure S1 of the Supporting Information. For each local minimum, a single-point energy calculation was done at the B3LYP/6-311G level of theory, and relative energies (in kcal/mol) calculated at this level of theory are listed in Figure S1 as well.

Up to 15 geometry-optimized dimer structures, including π-stacked and nonstacked dimers, were considered for each compound. For 1,4-naphthalenedicarboxylic acid, local minima for the monomer were found with C“C—C=O dihedral angles of approximately ±25 and ±155°, leading to the 6 local minima in Figure S1. These 4 possibilities for each carboxyl group would result in 256 possible nonstacked dimer structures to consider. However, chemical shift calculations performed on the monomer revealed that the conformations with dihedral angles of +25 and −25° led to similar chemical shifts, as did the

DOI: 10.1021/acs.jpcb.7b01465
J. Phys. Chem. B 2017, 121, 5086−5093

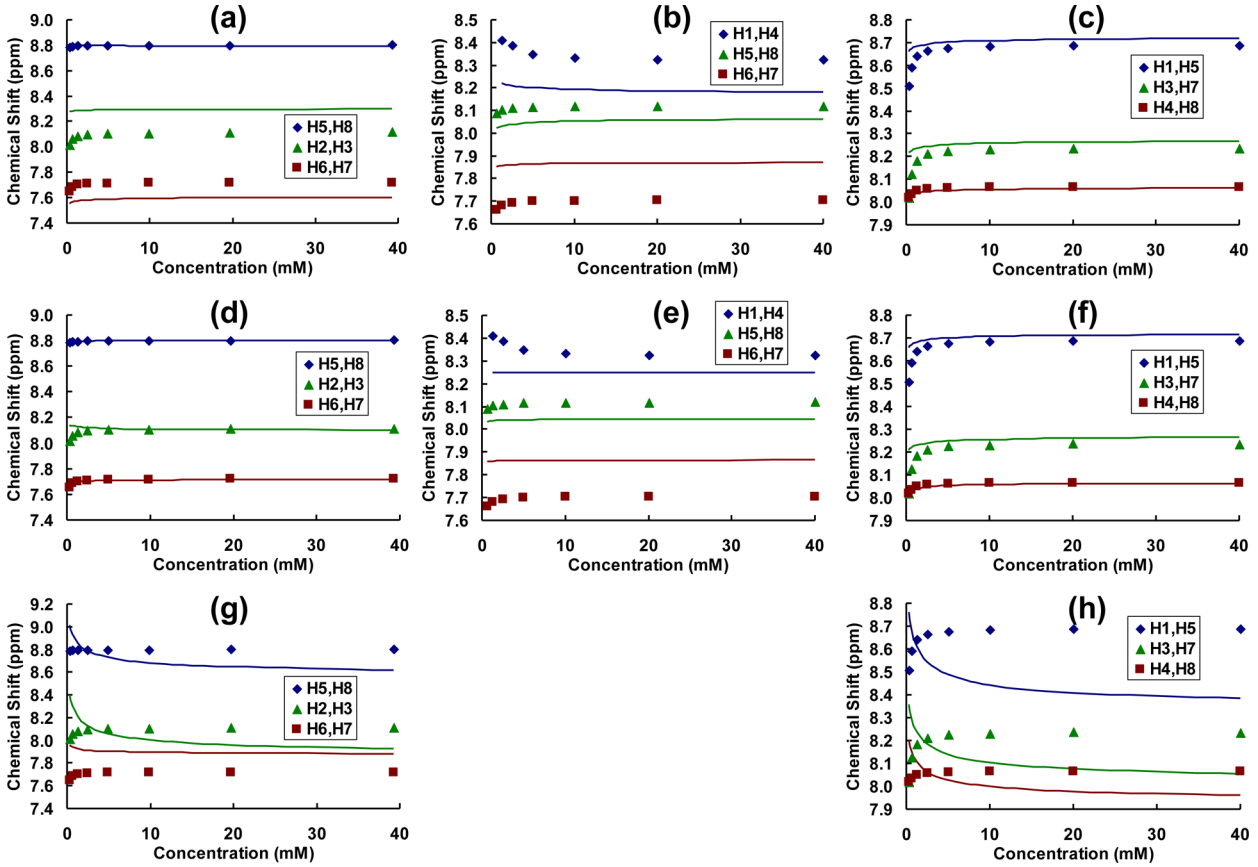

Figure 2. Experimental and calculated proton chemical shifts as a function of naphthalenedicarboxylic acid concentration. Diamonds, triangles, and squares are experimental data and solid lines are best-fit lines according to eq 2 with monomer and dimer chemical shifts determined from calculated chemical shifts of monomer and dimer structures weighted by one of three different methods as described in the text: (a, d, and g) 1,4-naphthalenedicarboxylic acid, (b and e) 2,3-naphthalenedicarboxylic acid, and (c, f, and h) 2,6-naphthalenedicarboxylic acid. In panels a–c, the monomer and dimer chemical shifts were determined from a Boltzmann weighted average of chemical shifts in all local minima structures. In panels d–f, monomer and dimer chemical shifts were determined from a weighted average that led to the best least-squares fit between the predicted and experimental proton chemical shifts. In panels g and h, the monomer structures were equally weighted, and only the stacked dimer structures were taken to contribute to the dimer chemical shift. The stacked dimer structures were also equally weighted.

two conformations with dihedral angles of +155 and −155°. This is similar to what was seen for different rotamers of 2-hydroxybenzoic acid and 2-aminobenzoic acid.[70] Therefore, only one case of either +25 or −25° and either +155 or −155° was considered, leading to 16 possibilities for nonstacked dimer structures. Due to symmetry, only 10 of these 16 possibilities resulted in a different structure, so 10 nonstacked dimers were considered for 1,4-naphthalenedicarboxylic acid. Five different stacked dimers were also considered. For 2,3-naphthalenedicarboxylic acid, only two nonstacked local minima were found for the dimer structure. For 2,6-naphthalenedicarboxylic acid, 10 nonstacked and 2 stacked local minima were found for the dimer structure. All dimers were confirmed to be local minima based on frequency calculations. The dimer structures that were considered are illustrated in Figure S1 along with their relative energies calculated at the B3LYP/6-311G level of theory.

Analysis. Assuming that the chemical shift of each proton at a particular concentration is a weighted average of the chemical shift of the monomer and dimer, the change in chemical shift with concentration for each proton can be predicted using the following equation:[30]

$$\delta_{obs} = \left[\frac{\left(\frac{-1+\sqrt{1+8KC_t}}{4K}\right)}{C_t}\right](\delta_m - \delta_d) + \delta_d \quad (2)$$

where δ_{obs} is the observed chemical shift at a total concentration C_t, K is the association constant for dimerization, and δ_m and δ_d are the chemical shifts of that proton in the monomer and dimer, respectively. Curves were fit to the experimental data by minimizing the squares of the differences between each experimental and predicted data point. As described below, average monomer and dimer shifts were calculated by Boltzmann weighting the calculated chemical shifts, by equally weighting only the π-stacked dimer structures, and by performing a full least-squares fit to determine the best weighting of the various monomer and dimer structures.

RESULTS AND DISCUSSION

Experimental ^{1}H chemical shifts are shown as a function of concentration for the three naphthalenedicarboxylic acids considered in Figure 2. Also shown in Figure 2 (as solid lines) are predicted chemicals shifts as a function of concentration using eq 2. In eq 2, the variable parameters are K, the association constant, and δ_m and δ_d, the monomer and

DOI: 10.1021/acs.jpcb.7b01465
J. Phys. Chem. B 2017, 121, 5086−5093

dimer chemical shifts, respectively. It was found that the value of K did not significantly affect the resulting fit, so a value of K = 1000 M^{-1} was used in all fits. This method is not expected to be a reliable way to determine the value of K.

The parameters that are most crucial to the quality of the fit in Figure 2 (vide infra) are the monomer and dimer chemical shifts. To extract an observed monomer and dimer chemical shift from the calculations, we assume a fast exchange between several low-energy structures. Chemical shifts were calculated for each geometry-optimized monomer and dimer structure, and averaging of these calculated chemical shifts was done in three ways: (a) Boltzmann weighting of all structures considered, (b) allowing the population of each structure to be determined by optimizing population of each structure to obtain the best fit with respect to experimental proton chemical shifts, and (c) assuming that the monomer structures contribute equally and considering only the π-stacked dimer structures also contributing equally.

From Figures 2a–c, a reasonable fit to the experimental proton chemical shifts measured at various concentrations was obtained by a Boltzmann weighting of all monomer and dimer structures. Notably, experiments indicate that all protons become less shielded (higher chemical shift) as the concentration increases with the exception of protons 1 and 4 of 2,3-naphthalenedicarboxylic acid. This trend is reproduced by the Boltzmann weighting: the calculations predict that all protons are less shielded in the weighted dimer chemical shift than in the weighted monomer chemical shift with the exception of protons 1 and 4 in 2,3-naphthalenedicarboxylic acid.

In addition to using the Boltzmann distribution and calculated energies to determine the relative contribution of each monomer and dimer structure, we also considered finding the weighting of the different monomer and dimer structures that leads to the best fit between experimental and calculated proton chemical shifts. The solid lines in Figures 2d–f are the predicted chemical shifts according to eq 2 by allowing the contribution of the various monomer and dimer structures to the overall monomer and dimer chemical shift to vary to minimize the difference of the squares of the predicted and experimental chemical shift of each proton at each concentration. As can be seen by comparing the first and second row of Figure 2, the agreement between experimental and calculated proton chemical shifts does not significantly improve when using the best least-squares fit to select the relative amount of each monomer and dimer structure that contributes to the overall chemical shift, as compared to Boltzmann weighting the monomer and dimer structures. This indicates that the Boltzmann weighting in fact does an excellent job reproducing the experimental chemical shifts, meaning that the agreement between experimental and calculated chemical shifts is consistent with the calculated energies.

For 1,4-naphthalenedicarboxylic acid, weighting the dimer structures according to a best fit between calculated and experimental chemical shifts leads to a weighted average that contains one stacked dimer, dimer 12 (see Supporting Information for dimer and monomer numbers) that contributes 30% to the overall dimer chemical shift. The rest of the contribution to the dimer chemical shifts of 1,4-naphthalenedicarboxylic acid consists of low-energy nonstacked dimer structures, including dimer 2 (29.7%), dimer 1 (23.1%), dimer 4 (12.2%), dimer 5 (3.4%), and dimer 6 (1.5%). As can be seen from Figure 2d, although the best-fit averaging reproduces the chemical shifts at high concentrations, inclusion of the stacked dimer does not reproduce the trend of protons 2 and 3 being less shielded in the dimer than in the monomer (increasing chemical shift at increasing concentrations). On the other hand, the Boltzmann weighting shown in Figure 2a does reproduce this trend. For 2,3-naphthalenedicarboxylic acid, no local minima were found corresponding to stacked dimer structures. The best least-squares fit leads to a weighted average of 88% dimer 2 and 12% dimer 1. Again, the best fit does not lead to a significant improvement in the agreement between calculated and experimental proton chemical shifts as compared to Boltzmann weighting the monomer and dimer structures, as can be seen by comparing Figures 2b and e. For 2,6-naphthalenedicarboxylic acid, the stacked dimers make only a minor contribution to the best-fit dimer structure (0.8% for dimer 11 and 0.05% for dimer 12), and the weighted average is comprised of a similar contribution of nonstacked dimers 5 (19%), 8 (18%), 4 (17%), 10 (13%), 6 (12%), 3 (8%), 2 (7%), and 9 (4%).

As can be seen from the energies in Figure S1, π-stacked dimer structures are much higher in energy than nonstacked dimer structures. Thus, Boltzmann weighting leads to an insignificant contribution to the weighted dimer chemical shift from the π-stacked structures. As mentioned in the introduction, π–π interaction energies are difficult to predict and generally require much higher-level calculations than those done in the present work. In particular, DFT does not accurately consider dispersion interactions, which are expected to contribute significantly to π–π-stacking interactions. As an illustration, energies of 1,4-naphthalenedicarboxylic acid dimers were calculated at the MP2/6-311G level of theory and are compared with the DFT-calculated energies in Table S1. The MP2 calculations predict energies of stacked dimers that are closer to those of nonstacked dimers than the B3LYP calculations, although the stacked dimer structures are still generally higher in energy than nonstacked dimers. Because we expect π-stacking to contribute to dimerization in naphthalenedicarboxylic acids, we also considered these π-stacked dimers in Figures 2g and h despite their higher calculated energy. In Figures 2g and h, only π-stacked dimers are included in the calculation of the overall dimer chemical shift. However, as can be seen from this figure, the agreement between calculation and experiment when only the π-stacked dimer structures are considered is quite bad. Thus, our experimental chemical shift changes are in agreement with the B3LYP/6-311G calculated energies for these three naphthalenedicarboxylic acids in that π-stacked dimer structures are not likely to contribute significantly to the overall structure. This is also in agreement with the trend of most protons becoming less shielded as the concentration of naphthalenedicarboxylic acid increases. If π-stacked dimers were predominant, ring current effects from the second naphthalene ring in the dimer would cause the majority of protons to experience a shielding effect, causing the proton chemical shifts to decrease with increasing concentration, the opposite of what is observed experimentally. This can also be seen by comparing the predicted and experimental proton chemical shifts in Figures 2(g and h). To increase confidence in these results, we performed chemical shift calculations at the MP2 level of theory with the same basis set and same B3LYP/6-31G* geometry-optimized structures for 1,4-naphthalenedicarboxylic acid as a representative case. These results are presented in the Supporting Information in Figure S2. The MP2-calculated proton chemical shifts also indicate that

DOI: 10.1021/acs.jpcb.7b01465
J. Phys. Chem. B 2017, 121, 5086–5093

Table 1. Experimental Carbon Chemical Shifts

1,4-naphthalenedicarboxylic acid				2,3-naphthalenedicarboxylic acid				2,6-naphthalenedicarboxylic acid			
carbon	40 mM	2 mM	1 mM	carbon	40 mM	2 mM	1 mM	carbon	40 mM	2 mM	1 mM
C=O	168.413	168.401	168.414	C=O	168.672	168.640	168.633	C=O	167.162	167.153	167.156
C9,C10	132.219			C9,C10	132.758	132.750	132.753	C9,C10	134.121	134.113	134.107
C1,C4	130.664	130.653	130.657	C2,C3	129.834	129.858	129.879	C1,C5	130.141	130.127	130.116
C2,C3	127.786	127.766	127.749	C1,C4	129.073			C2,C6	130.080	130.086	130.082
C6,C7	127.514	127.498	127.475	C5,C8	128.507	128.494	128.493	C3,C7	129.693	129.684	129.671
C5,C8	125.829	125.821	125.829	C6,C7	128.389	128.369	128.363	C4,C8	125.869	125.863	125.864

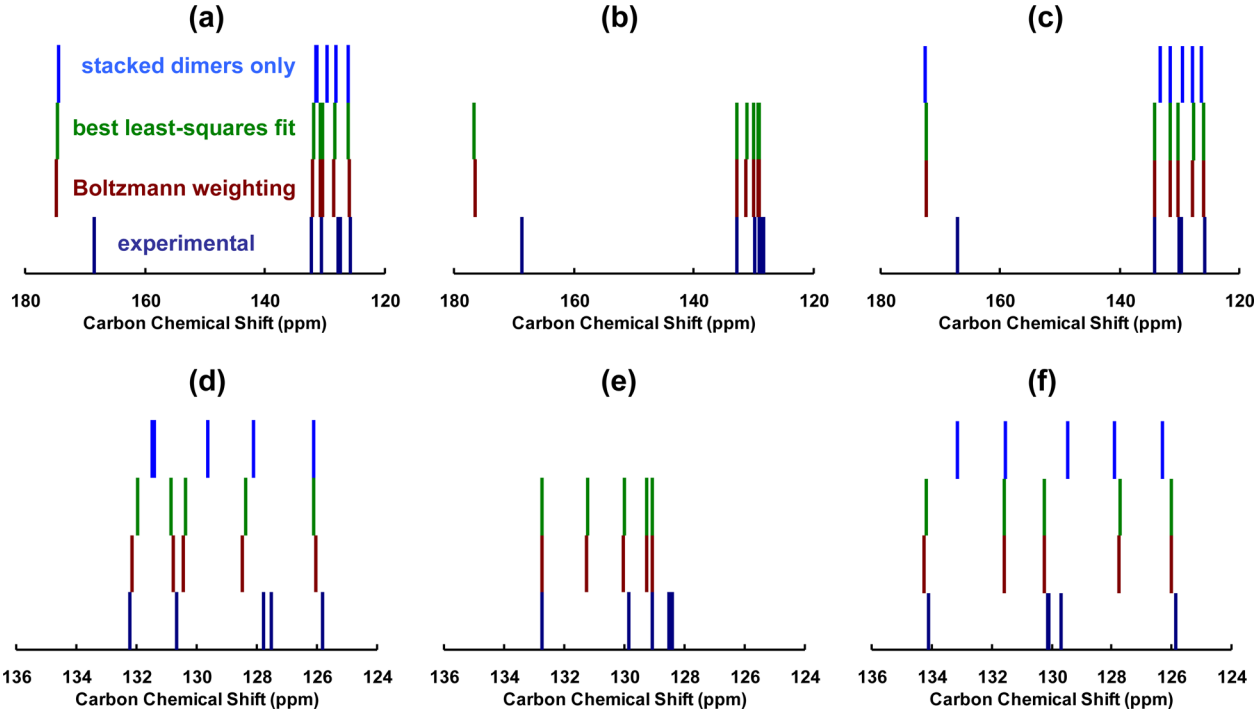

Figure 3. Stick spectra containing experimental and calculated carbon chemical shifts: (a and d) 1,4-naphthalenedicarboxylic acid, (b and e) 2,3-naphthalenedicarboxylic acid, and (c and f) 2,6-naphthalenedicarbxylic acid. Panels d–f are expanded versions of panels a–c, focusing on the aromatic carbon region. In each graph, the lowest row (dark blue) is a stick spectrum containing the experimental chemical shifts at 40 mM concentration; the second row (red) is a stick spectrum of the Boltzmann-weighted dimer chemical shifts, and the third row (green) is a stick spectrum of the best least-squares fit dimer chemical shifts. The top row (light blue) is a stick spectrum containing the average dimer chemical shifts of the stacked dimers only.

Boltzmann weighting or weighting according to a best fit to experimental proton chemical shifts does a good job at reproducing the experimental trends, while considering only stacked dimer structures does not.

Carbon chemical shifts of the three naphthalenedicarboxylic acid isomers at concentrations of 40, 2, and 1 mM are listed in Table 1. The carbon chemical shifts do not change significantly with concentration, shifting by at most 0.05 ppm between the highest and lowest concentrations. This is also an indication that stacked dimers do not contribute significantly to the structure of these naphthalenedicarboxylic acids because stacked structures would lead to ring current effects that would increase the shielding of the aromatic carbons. Calculated carbon chemical shifts of the dimers are considered in Figure 3. Carbon chemical shifts calculated at the MP2 level of theory are also included for 1,4-naphthalenedicarboxylic acid in Figure S3. For each isomer of naphthalenedicarboxylic acid, experimental carbon chemical shifts at 40 mM concentration, calculated dimer chemical shifts using Boltzmann weighting of all monomer and dimer structures, calculated dimer chemical shifts using the best-fit weighting, and calculated chemical shifts considering only π-stacked dimers are shown. In each case, the agreement between calculated and experimental ^{13}C chemical shifts does not strongly depend on the averaging method used.

CONCLUSIONS

Both single-point energy calculations and comparisons between experimental and calculated proton chemical shifts indicate that π-stacked dimers are not as important as non-π-stacked dimers in the three isomers of naphthalenedicarboxylic acid considered in this work. This is in contrast to our initial expectations; although we anticipated that carboxylic acid dimer formation would be more important than π-stacking, we expected that dimer structures incorporating both stabilizing effects would be lower in energy and closer to the true dimer structure than those structures that contained only carboxylic dimer formation. However, from the geometry-optimized structures shown in Figure S1, it appears that in the stacked structures and formation of carboxylic acid dimers results in distortion of the naphthalene ring. This distortion to form the carboxylic acid

DOI: 10.1021/acs.jpcb.7b01465
J. Phys. Chem. B 2017, 121, 5086–5093

dimer presumably results in an increase in energy that offsets any additional stabilization afforded by the $\pi-\pi$ interactions.

The methods we used in this study can have broad applications in the study of self-association in other similar compounds. We used fairly straightforward DFT calculations employing a widely available functional and small basis sets. The dimer geometry optimizations at this level of theory usually took less than 24 h using 8 CPU processors, and the dimer chemical shift calculations were complete within approximately 35 min. However, despite the ease of the calculations, the resulting calculated monomer and dimer chemical shifts were generally in good agreement with experimental chemical shifts, and when they were not in agreement, it allowed us to select between dimer structures that were likely to contribute to the true structure in solution (e.g., nonstacked dimers) and those that were not likely to contribute significantly to the true structure (stacked dimers in this case). As expected, the structure of a molecule in solution can best be modeled by a weighted average of several low-energy structures that are populated according to the Boltzmann distribution and the predicted relative energies of each structure. By weighting the calculated chemical shifts for each structure accordingly, we obtained a good agreement between experimental and calculated chemical shifts.

This study considered changes in proton chemical shifts rather than changes in carbon chemical shifts as in our previous studies.[30,31] This has the advantage that proton chemical shifts are more easily measured due to the large gyromagnetic ratio and natural abundance of the ^{1}H nucleus. Although carbon chemical shifts are generally more reliably predicted by computational methods due to carbon having a larger chemical shift dispersion and being less influenced by solvent effects, measuring carbon spectra, especially for compounds containing slowly relaxing nonprotonated carbons, takes orders of magnitude more time. We showed here that proton chemical shifts predicted by rather standard DFT methods can reliably reproduce experimental monomer and dimer chemical shifts in naphthalenedicarboxylic acids.

■ ASSOCIATED CONTENT

Supporting Information

The Supporting Information is available free of charge on the ACS Publications website at DOI: 10.1021/acs.jpcb.7b01465.

Monomer and dimer structures labeled with dihedral angles, degeneracy, and relative energy (in kcal/mol calculated at the B3LYP/6-311G level of theory); MP2-calculated energies and chemical shifts for 1,4-naphthalenedicarboxylic acid; and complete ref 57 (PDF)

■ AUTHOR INFORMATION

Corresponding Author

*E-mail: lcasabi@clemson.edu.

ORCID

Leah B. Casabianca: 0000-0001-9447-3236

Present Address

‡P.D.G.: Department of Chemistry, Emory University, Atlanta, GA 30322, United States.

Notes

The authors declare no competing financial interest.

■ ACKNOWLEDGMENTS

The authors thank Dr. John Glushka for help collecting the ^{13}C NMR spectra. The chemical shift calculations were made possible thanks to computing time on Clemson University's Palmetto Cluster. This work was supported by Clemson University start-up funds.

■ REFERENCES

(1) Liang, P.-C.; Liu, H.-K.; Yeh, C.-T.; Lin, C.-H.; Zima, V. Supramolecular Assembly of Calcium Metal-Organic Frameworks with Structural Transformations. *Cryst. Growth Des.* **2011**, *11*, 699−708.

(2) Loiseau, T.; Mellot-Draznieks, C.; Muguerra, H.; Ferey, G.; Haouas, M.; Taulelle, F. Hydrothermal Synthesis and Crystal Structure of a New Three-Dimensional Aluminum-Organic Framework MIL-69 with 2,6-Naphthalenedicarboxylate (ndc), Al(OH) (ndc)·H2O. *C. R. Chim.* **2005**, *8*, 765−772.

(3) Jiang, Z. Trinuclear Manganese Metal-Organic Frameworks Based on 2,6-Naphthalenedicarboxylic Acid. *Asian J. Chem.* **2013**, *25*, 2347−2348.

(4) Zhang, Y.; Wang, X.; Li, S.; Song, B.; Shao, K.; Su, Z. Ligand-Directed Assembly of Polyoxovanadate-Based Metal−Organic Polyhedra. *Inorg. Chem.* **2016**, *55*, 8770−8775.

(5) Moon, H. R.; Kobayashi, N.; Suh, M. P. Porous Metal-Organic Framework with Coordinatively Unsaturated Mn-II Sites: Sorption Properties for Various Gases. *Inorg. Chem.* **2006**, *45*, 8672−8676.

(6) Park, H.; Britten, J. F.; Mueller, U.; Lee, J.; Li, J.; Parise, J. B. Synthesis, Structure Determination, and Hydrogen Sorption Studies of New Metal-Organic Frameworks Using Triazole and Naphthalenedicarboxylic Acid. *Chem. Mater.* **2007**, *19*, 1302−1308.

(7) Sapchenko, S. A.; Dybtsev, D. N.; Samsonenko, D. G.; Belosludov, R. V.; Belosludov, V. R.; Kawazoe, Y.; Schroder, M.; Fedin, V. P. Selective Gas Adsorption in Microporous Metal-Organic Frameworks Incorporating Urotropine Basic Sites: An Experimental and Theoretical Study. *Chem. Commun.* **2015**, *51*, 13918−13921.

(8) Lin, H.; Rong, X.; Liu, G.; Wang, X.; Wang, X.; Duan, S. Fluorescent Sensing and Electrocatalytic Properties of Three Zn(II)/Co(II) Coordination Complexes Containing Two Different Dicarboxylates and Two Various Bis(pyridyl)-bis(amide) Ligands. *J. Mol. Struct.* **2016**, *1119*, 396−403.

(9) Meng, B.; Liu, Y.; Xing, Y.; Wang, X.; Li, W. Octanuclear Zinc(II) Carboxylate Framework Based on 1,4-Naphthalenedicarboxylic Acid. *Inorg. Chem. Commun.* **2016**, *73*, 142−146.

(10) Che, G.-B.; Xu, M.-L.; Liu, C.-B.; Wang, Q.-W.; Xu, Z.-L. Synthesis, Crystal Structure and Characterization of a Cobalt Coordination Polymer: [Co(1,4-ndc)(L)(H2O)]n. *Chin. J. Struct. Chem.* **2008**, *27*, 773−776.

(11) Lu, Y.-B.; Jin, S.; Zhou, Z.-G.; Zhang, S.-Y.; Lou, G. T.; Xie, Y.-R. The Syntheses, Structures, Magnetic and Luminescent Properties of Five New Lanthanide(III)-2,6-Naphthalenedicarboxylate Complexes. *Inorg. Chem. Commun.* **2014**, *48*, 73−76.

(12) Lu, Y.-B.; Chen, L.-P.; Zhang, S.-Y.; Lian, P.; Xie, Y.-R. The Syntheses, Structures, and Magnetic Properties of Four 2D Lanthanide(III)-Naphthalenedicarboxylic Complexes. *Z. Anorg. Allg. Chem.* **2015**, *641*, 2408−2413.

(13) Lin, H.-Y.; Lu, H.; Le, M.; Jian, L.; Wang, X.-L.; Liu, G.; Zhang, J. Effect of Three Bis-pyridyl-bis-Amide Ligands with Various Spacers on the Structural Diversity of New Multifunctional Cobalt(II) Coordination Polymers. *J. Solid State Chem.* **2015**, *226*, 66−73.

(14) Shan, N.; Bond, A. D.; Jones, W. Crystal Engineering Using 4,4'-bipyridyl with Di- and Tricarboxylic Acids. *Cryst. Eng.* **2002**, *5*, 9−24.

(15) Guo, X.-G.; Yang, W.-B.; Wu, X.-Y.; Lin, L.; Lu, C.-Z. 3D/3D Hetero-Interpenetrating Diamondoid Framework and Homo-Interpenetrating pcu Network by a One-Pot Reaction. *Eur. J. Inorg. Chem.* **2014**, *15*, 2481−2485.

(16) Mullins, O. C. The Asphaltenes. *Annu. Rev. Anal. Chem.* **2011**, *4*, 393−418.

(17) Gordeev, E. G.; Polynski, M.; Ananikov, V. P. Fast and Accurate Computational Modeling of Adsorption on Graphene: A Dispersion

DOI: 10.1021/acs.jpcb.7b01465
J. Phys. Chem. B 2017, 121, 5086−5093

Interaction Challenge. *Phys. Chem. Chem. Phys.* **2013**, *15*, 18815−18821.
(18) An, Y.; Raju, R. K.; Lu, T.; Wheeler, S. E. Aromatic Interactions Modulate the 5′-Base Selectivity of the DNA-Binding Autoantibody ED-10. *J. Phys. Chem. B* **2014**, *118*, 5653−5659.
(19) Hargis, J. C.; Schaefer, H. F., III; Houk, K. N.; Wheeler, S. E. Noncovalent Interactions of a Benzo[a]pyrene Diol Epoxide with DNA Base Pairs: Insight into the Formation of Adducts of (+)-BaP DE-2 with DNA. *J. Phys. Chem. A* **2010**, *114*, 2038−2044.
(20) Burley, S. K.; Petsko, G. A. Aromatic-Aromatic Interaction: A Mechanism of Protein Structure Stabilization. *Science* **1985**, *229*, 23−28.
(21) Ringer, A. L.; Sherrill, C. D. Substituent Effects in Sandwich Configurations of Multiply Substituted Benzene Dimers Are Not Solely Governed By Electrostatic Control. *J. Am. Chem. Soc.* **2009**, *131*, 4574−4575.
(22) Wheeler, S. E.; Bloom, J. W. G. Toward a More Complete Understanding of Noncovalent Interactions Involving Aromatic Rings. *J. Phys. Chem. A* **2014**, *118*, 6133−6147.
(23) Geng, Y.; Takatani, T.; Hohenstein, E. G.; Sherrill, C. D. Accurately Characterizing the $\pi-\pi$ Interaction Energies of Indole−Benzene Complexes. *J. Phys. Chem. A* **2010**, *114*, 3576−3582.
(24) Parker, T. M.; Hohenstein, E. G.; Parrish, R. M.; Hud, N. V.; Sherrill, C. D. Quantum-Mechanical Analysis of the Energetic Contributions to π Stacking in Nucleic Acids versus Rise, Twist, and Slide. *J. Am. Chem. Soc.* **2013**, *135*, 1306−1316.
(25) Parrish, R. M.; Sherrill, C. D. Quantum-Mechanical Evaluation of $\pi-\pi$ versus Substituent−π Interactions in π Stacking: Direct Evidence for the Wheeler−Houk Picture. *J. Am. Chem. Soc.* **2014**, *136*, 17386−17389.
(26) Raju, R. K.; Bloom, J. W. G.; Wheeler, S. E. Broad Transferability of Substituent Effects in π-Stacking Interactions Provides New Insights into Their Origin. *J. Chem. Theory Comput.* **2013**, *9*, 3479−3490.
(27) Wheeler, S. E. Local Nature of Substituent Effects in Stacking Interactions. *J. Am. Chem. Soc.* **2011**, *133*, 10262−10274.
(28) Wheeler, S. E. Understanding Substituent Effects in Noncovalent Interactions Involving Aromatic Rings. *Acc. Chem. Res.* **2013**, *46*, 1029−1038.
(29) da Costa, L. M.; Stoyanov, S. R.; Gusarov, S.; Seidl, P. R.; Walkimar de Carneiro, J.; Kovalenko, A. Computational Study of the Effect of Dispersion Interactions on the Thermochemistry of Aggregation of Fused Polycyclic Aromatic Hydrocarbons as Model Asphaltene Compounds in Solution. *J. Phys. Chem. A* **2014**, *118*, 896−908.
(30) Casabianca, L. B.; de Dios, A. C. ^{13}C NMR Study of the Self-Association of Chloroquine, Amodiaquine, and Quinine. *J. Phys. Chem. A* **2004**, *108*, 8505−8513.
(31) Casabianca, L. B.; de Dios, A. C. Interactions Between Pairs of Antimalarial Drugs Studied by Experimental and Ab Initio ^{13}C NMR Chemical Shifts. *Magn. Reson. Chem.* **2006**, *44*, 276−282.
(32) Houbiers, C.; Lima, J. C.; Maçanita, A. L.; Santos, H. Color Stabilization of Malvidin 3-Glucoside: Self-Aggregation of the Flavylium Cation and Copigmentation with the Z-Chalcone Form. *J. Phys. Chem. B* **1998**, *102*, 3578−3585.
(33) Briffitt, R.; Day, I. J. Influence of Structural Isomerism and Fluorine Atom Substitution on the Self-Association of Naphthoic Acid. *J. Phys. Chem. B* **2015**, *119*, 6703−6710.
(34) D'Amelio, N.; Aroulmoji, V.; Toraldo, A.; Sundaraganesan, N.; Anbarasan, P. M. Aggregation Properties and Structural Studies of Anticancer Drug Irinotecan in DMSO Solution Based on NMR Measurements. *J. Mol. Struct.* **2012**, *1013*, 26−35.
(35) Rodríguez-Abreu, C.; Torres, C. A.; Tiddy, G. J. T. Chromonic Liquid Crystalline Phases of Pinacyanol Acetate: Characterization and Use as Templates for the Preparation of Mesoporous Silica Nanofibers. *Langmuir* **2011**, *27*, 3067−3073.
(36) Rodríguez-Abreu, C.; Torres, C. A.; Solans, C.; López-Quintela, A.; Tiddy, G. J. T. Characterization of Perylene Diimide Dye Self-Assemblies and Their Use As Templates for the Synthesis of Hybrid and Supermicroporous Nanotubules. *ACS Appl. Mater. Interfaces* **2011**, *3*, 4133−4141.
(37) Ruso, J. M.; Taboada, P.; Attwood, D.; Mosquera, V.; Sarmiento, F. Determination of the Aggregation Properties of Weakly Self-Associating Systems by NMR Techniques: The Self-Association of Propranolol Hydrochloride in Aqueous Electrolyte Solution. *Phys. Chem. Chem. Phys.* **2000**, *2*, 1261−1265.
(38) Taboada, P.; Attwood, D.; Ruso, J. M.; García, M.; Sarmiento, F.; Mosquera, V. Self Association of the Penicillin Sodium Nafcillin in Aqueous Solution. *Langmuir* **2000**, *16*, 3175−3181.
(39) Xiao, C.; Wu, M.; Zhang, Y.; Zhao, X.; Yu, J. The Structure-Dependent Self-Association of Five Phenolic Acids in Aqueous Solution. *Magn. Reson. Chem.* **2014**, *52*, 460−466.
(40) Zhang, Y.; Xiang, J.; Tang, Y.; Xu, G.; Yan, W. Aggregation Behaviour of Two Thiacarbocyanine Dyes in Aqueous Solution. *Dyes Pigm.* **2008**, *76*, 88−93.
(41) Harrison, W. J.; Mateer, D. L.; Tiddy, G. J. T. Liquid-Crystalline J-Aggregates Formed by Aqueous Ionic Cyanine Dyes. *J. Phys. Chem.* **1996**, *100*, 2310−2321.
(42) Renshaw, M. P.; Day, I. J. NMR Characterization of the Aggregation State of the Azo Dye Sunset Yellow in the Isotropic Phase. *J. Phys. Chem. B* **2010**, *114*, 10032−10038.
(43) Katz, J. R.; Day, I. J. Investigating the Interaction of Sunset Yellow Aggregates and 6-Fluoro-2-Naphthoic Acid: Increasing Probe Molecule Complexity. *Magn. Reson. Chem.* **2014**, *52*, 435−439.
(44) Katz, J. R.; Day, L. J.; Day, I. J. NMR Investigations of the Interaction Between the Azo-Dye Sunset Yellow and Fluorophenol. *J. Phys. Chem. B* **2013**, *117*, 11793−11800.
(45) Bradley, J. P.; Velaga, S. P.; Antzutkin, O. N.; Brown, S. P. Probing Intermolecular Crystal Packing in γ-Indomethacin by High-Resolution ^{1}H Solid-State NMR Spectroscopy. *Cryst. Growth Des.* **2011**, *11*, 3463−3471.
(46) Ganapathy, S.; Sengupta, S.; Wawrzyniak, P. K.; Huber, V.; Buda, F.; Baumeister, U.; Würthner, F.; de Groot, H. J. M. Zinc Chlorins for Artificial Light-Harvesting Self-Assemble Into Antiparallel Stacks Forming a Microcrystalline Solid-State Material. *Proc. Natl. Acad. Sci. U. S. A.* **2009**, *106*, 11472−11477.
(47) Spiess, H. W. Magic Angle Spinning NMR of Macromolecular and Supramolecular Systems. *Isr. J. Chem.* **2014**, *54*, 16−24.
(48) Fischbach, I.; Pakula, T.; Minkin, P.; Fechtenkotter, A.; Mullen, K.; Spiess, H. W.; Saalwachter, K. Structure and Dynamics in Columnar Discotic Materials: A Combined X-ray and Solid-State NMR Study of Hexabenzocoronene Derivatives. *J. Phys. Chem. B* **2002**, *106*, 6408−6418.
(49) Pandit, A.; Ocakoglu, K.; Buda, F.; van Marle, T.; Holzwarth, A. R.; de Groot, H. J. M. Structure Determination of a Bio-Inspired Self-Assembled Light-Harvesting Antenna by Solid-State NMR and Molecular Modeling. *J. Phys. Chem. B* **2013**, *117*, 11292−11298.
(50) Uemura, T.; Uchida, N.; Asano, A.; Saeki, A.; Seki, S.; Tsujimoto, M.; Isoda, S.; Kitagawa, S. Highly Photoconducting Pi-Stacked Polymer Accommodated in Coordination Nanochannels. *J. Am. Chem. Soc.* **2012**, *134*, 8360−8363.
(51) Strohmeier, M.; Orendt, A. M.; Alderman, D. W.; Grant, D. M. Investigation of the Polymorphs of Dimethyl-3,6-dichloro-2,5-dihydroxyterephthalate by C-13 Solid-State NMR Spectroscopy. *J. Am. Chem. Soc.* **2001**, *123*, 1713−1722.
(52) Hudson, Z. M.; Sun, C.; Harris, K. J.; Lucier, B. E. G.; Schurko, R. W.; Wang, S. N. Probing the Structural Origins of Vapochromism of a Triarylboron-Functionalized Platinum(II) Acetylide by Optical and Multinuclear Solid-State NMR Spectroscopy. *Inorg. Chem.* **2011**, *50*, 3447−3457.
(53) Mafra, L.; Paz, F. A. A.; Shi, F.-N.; Ferreira, R. A. S.; Carlos, L. D.; Trindade, T.; Fernandez, C.; Klinowski, J.; Rocha, J. Crystal Structure, Solid-state NMR Spectroscopic and Photoluminescence Studies of Organic-Inorganic Hybrid Materials (HL)(6)[Ge-6(OH)(6) (hedp)(6)]·2(L)·nH(2)O, L = hqn or phen. *Eur. J. Inorg. Chem.* **2006**, *23*, 4741−4751.
(54) Majumdar, R. D.; Gerken, M.; Hazendonk, P. Solid-State ^{1}H and ^{13}C Nuclear Magnetic Resonance Spectroscopy of Athabasca Oil

DOI: 10.1021/acs.jpcb.7b01465
J. Phys. Chem. B 2017, 121, 5086−5093

Sands Asphaltenes: Evidence for Interlocking π-Stacked Nanoaggregates with Intercalated Alkyl Side Chains. *Energy Fuels* **2015**, *29*, 2790−2800.
(55) Brown, S. P.; Schnell, I.; Brand, J. D.; Müllen, K.; Spiess, K. W. The Competing Effects of π-π Packing and Hydrogen Bonding in a Hexabenzocoronene Carboxylic Acid Derivative: A ^{1}H Solid-State MAS NMR Investigation. *Phys. Chem. Chem. Phys.* **2000**, *2*, 1735−1745.
(56) Sklenář, V.; Bax, A. Two-Dimensional Heteronuclear Chemical-Shift Correlation in Proteins at Natural Abundance ^{15}N and ^{13}C levels. *J. Magn. Reson.* **1987**, *71*, 379−383.
(57) Frisch, M. J.; Trucks, G. W.; Schlegel, H. B.; Scuseria, G. E.; Robb, M. A.; Cheeseman, J. R.; Scalmani, G.; Barone, V.; Mennucci, B.; Petersson, G. A.; et al. *Gaussian 09*, revision B.01; Gaussian, Inc.: Wallingford, CT, 2009.
(58) Becke, A. D. Density-Functional Thermochemistry. III. The Role of Exact Exchange. *J. Chem. Phys.* **1993**, *98*, 5648−5652.
(59) Lee, C.; Yang, W.; Parr, R. G. Development of the Colle-Salvetti Correlation-Energy Formula Into a Functional of the Electron Density. *Phys. Rev. B: Condens. Matter Mater. Phys.* **1988**, *37*, 785−789.
(60) Hehre, W. J.; Ditchfield, R.; Pople, J. A. Self-Consistent Molecular Orbital Methods. 12. Further Extensions of Gaussian-Type Basis Sets for Use in Molecular-Orbital Studies of Organic-Molecules. *J. Chem. Phys.* **1972**, *56*, 2257.
(61) Krishnan, R.; Binkley, J. S.; Seeger, R.; Pople, J. A. Self-Consistent Molecular Orbital Methods. XX. A basis set for correlated wave functions. *J. Chem. Phys.* **1980**, *72*, 650−654.
(62) Ditchfield, R. Self-Consistent Perturbation Theory of Diamagnetism. 1. Gauge-Invariant LCAO Method for N.M.R. Chemical Shifts. *Mol. Phys.* **1974**, *27*, 789−807.
(63) Miertuš, S.; Scrocco, E.; Tomasi, J. Electrostatic Interaction of a Solute with a Continuum. A Direct Utilization of Ab Initio Molecular Potentials for the Prevision of Solvent Effects. *Chem. Phys.* **1981**, *55*, 117−129.
(64) Miertuš, S.; Tomasi, J. Approximate Evaluations of the Electrostatic Free Energy and Internal Energy Changes in Solution Processes. *Chem. Phys.* **1982**, *65*, 239−245.
(65) Pascual-Ahuir, J. L.; Silla, E.; Tuñón, I. GEPOL: An Improved Description of Molecular-Surfaces. 3. A New Algorithm for the Computation of a Solvent-Excluding Surface. *J. Comput. Chem.* **1994**, *15*, 1127−1138.
(66) Tomasi, J.; Mennucci, B.; Cammi, R. Quantum Mechanical Continuum Solvation Models. *Chem. Rev.* **2005**, *105*, 2999−3093.
(67) Gottlieb, H. E.; Kotlyar, V.; Nudelman, A. NMR Chemical Shifts of Common Laboratory Solvents as Trace Impurities. *J. Org. Chem.* **1997**, *62*, 7512−7515.
(68) Zurek, E.; Pickard, C. J.; Walczak, B.; Autschbach, J. Density Functional Study of the ^{13}C NMR Chemical Shifts in Small-to-Medium-Diameter Infinite Single-Walled Carbon Nanotubes. *J. Phys. Chem. A* **2006**, *110*, 11995−12004.
(69) Marques, M. A. L.; d'Avezac, M.; Mauri, F. Magnetic Response and NMR Spectra of Carbon Nanotubes from *Ab Initio* Calculations. *Phys. Rev. B: Condens. Matter Mater. Phys.* **2006**, *73*, 125433.
(70) Burnette, R. R.; Weinhold, F. Determination of the Conformation of 2-Hydroxy- and 2-Aminobenzoic Acid Dimers Using ^{13}C NMR and Density Functional Theory/Natural Bond Order Analysis: The Central Importance of the Carboxylic Acid Carbon. *J. Phys. Chem. A* **2006**, *110*, 8832−8839.

DOI: 10.1021/acs.jpcb.7b01465
J. Phys. Chem. B 2017, 121, 5086−5093